Utilizing Cellulose and Lignin Derivatives in Green Packaging: Development of *Syzygium aromaticum* Essential Oil-Loaded Antibacterial and UV-Blocking Materials

Naile Angın *

* *Corresponding author: naile.angin@btu.edu.tr*

DOI: 10.15376/biores.21.4.9861-9879

GRAPHICAL ABSTRACT

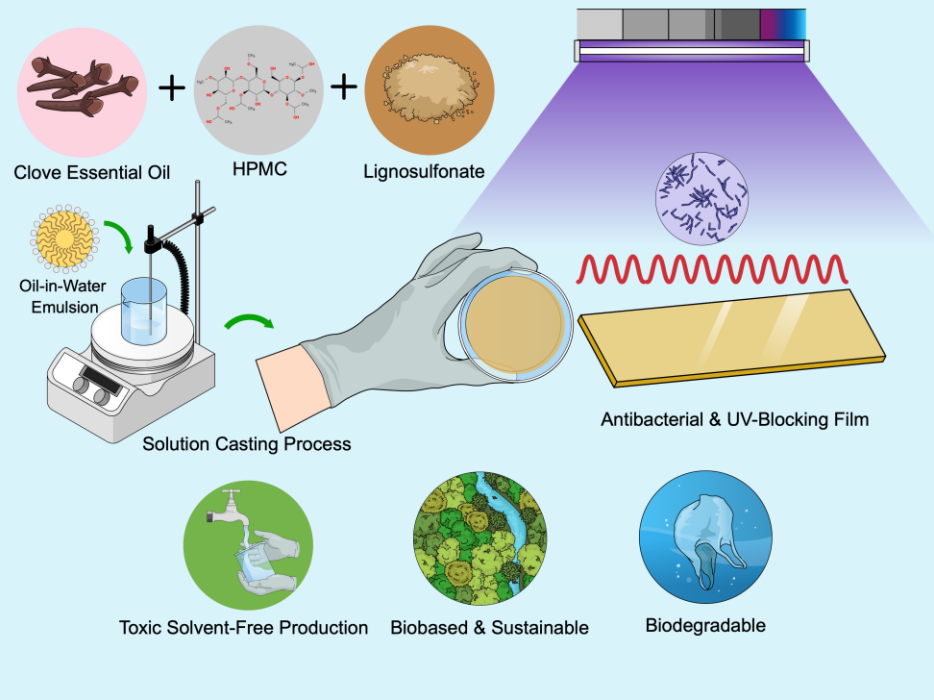

Utilizing Cellulose and Lignin Derivatives in Green Packaging: Development of *Syzygium aromaticum* Essential Oil-Loaded Antibacterial and UV-Blocking Materials

Naile Angın *

The environmental impact of long-lasting conventional plastics and related microplastic pollution have created an urgent need for sustainable packaging alternatives. Multifunctional green packaging films were developed by incorporating calcium lignosulfonate (CaLS) and clove (*Syzygium aromaticum*) essential oil emulsion (SAEO) into a hydroxypropyl methylcellulose (HPMC) matrix. Films were prepared by the aqueous solution casting method at different SAEO concentrations. The chemical profile of the essential oil was determined by GC-MS analysis, confirming eugenol as the major component (86.9%). The structural, thermal, mechanical, color, and selected functional properties of the films were characterized. CaLS incorporation increased tensile strength by approximately 9% compared to neat HPMC. The addition of SAEO reduced tensile strength while enhancing flexibility. CaLS remarkably enhanced UV-blocking performance of HPMC from 55% to 98%, which was slightly decreased to 94% following SAEO addition. Antibacterial activity increased with essential oil concentration, particularly the film containing 6 wt.%. SAEO achieving approximately 99% reduction against *Escherichia coli* and 70% against *Staphylococcus aureus*. The findings suggest that the combined use of cellulose and lignin derivatives with clove essential oil offers an integrated approach for the development of multifunctional food packaging materials, as well as providing a field of application for non-wood forest products.

DOI: 10.15376/biores.21.4.9861-9879

Keywords: Cellulose derivatives; Lignin; Clove essential oil; HPMC film; Non-wood forest products

*Contact information: Department of Forest Industry Engineering, Bursa Technical University, 16300, Bursa, TÜRKİYE; and Furniture and Wood Application and Research Center, Bursa Technical University, 16310 Bursa, TÜRKİYE; *Email: naile.angin@btu.edu.tr*

INTRODUCTION

The packaging industry has been using petroleum-based synthetic polymers for many years. However, global plastic consumption is expected to nearly triple by 2060, which will further worsen the ecological crisis caused by fossil-fuel-derived materials (Stoica *et al*. 2024). Single-use packaging is one of the major contributors to this pollution. After being thrown away, these materials can remain in the environment for centuries without degradation, and over time, they break down into microplastics and even smaller nanoplastics that contaminate the food chain and accumulate in living organisms (Ncube *et al*. 2020). Owing to their smaller size, nanoplastics can cross biological barriers and are therefore associated with greater ecotoxicological hazards and human health concerns (Xu

et al. 2022). To address these concerns, research is increasingly focused on biodegradable options derived from renewable sources and agricultural industrial waste. Changes in legacy, including the EU's directive on single-use plastics and FDA standards for food packaging materials, are accelerating this movement by imposing stricter environmental requirements (Guo *et al*. 2025).

Cellulose and lignin derivatives are promising candidates for sustainable film packaging solutions thanks to their natural origin, abundance, and relatively low cost (Erişir and Gümüşkaya 2024; Verma *et al*. 2024; Zor *et al*. 2024). Hydroxypropyl methylcellulose (HPMC), one of the most important cellulose derivatives, is frequently preferred due to its superior potential for film formation and permeability traits, and its biocompatible structure allows for safe use in various applications involving contact with the human body and food (Otoni *et al*. 2018; Tundisi *et al*. 2021; Mobilawon *et al*. 2025). Lignin and its derivatives offer significant advantages as a natural polymer and functional additive that enhances the properties of packaging material (Tribot *et al*. 2019). The incorporation of lignin into various packaging formulations has shown great potential for improving mechanical, thermal, and barrier properties while contributing to biodegradability and reducing environmental impact (Shi and Li 2016). Inspired by the structural composition of wood which contains both cellulose and lignin, the combined application of their derivatives allows for the creation of hybrid packaging systems capable of fulfilling specific performance criteria simultaneously.

Packaging materials are required to meet essential performance criteria, such as offering a UV barrier and having antibacterial characteristics. The UV barrier helps maintain product stability by reducing photodegradation, oxidation, color change, and loss of active ingredients in light-sensitive products. This feature offers a significant advantage in extending shelf life and maintaining product quality in active packaging applications (Tripathi *et al*. 2024). In this study, calcium-lignosulfonate (CaLS) was chosen to enhance the UV barrier properties of HPMC base matrix. CaLS is a lignin derivative obtained as a byproduct of the sulfite pulping process. The strongly ionized sulfonate groups along its lignin backbone confer hydrophilicity and good water solubility (Tang *et al*. 2023). A previous study reported that films produced with microcrystalline cellulose and lignosulfonate exhibited excellent UV shielding properties and blocked all irradiation in the UVB-UVC regions (Guo *et al*. 2023). Furthermore, the literature also contains findings indicating that lignosulfonate exhibits limited antimicrobial properties (Reyes *et al*. 2024; Jha and Kumar 2025). However, these features must be supported with enhanced antibacterial properties to ensure packaging safety. Therefore, essential oils can be used to give the packaging active protective properties as a natural solution (Atarés and Chiralt 2016; Sharma *et al*. 2021). Essential oils are used as active phases in packaging formulations due to their rich monoterpene content and broad-spectrum antibacterial activity. Active packaging films that integrate essential oils have demonstrated effectiveness in extending the shelf life of various food products, including meat, fruits and vegetables. These films help maintain the freshness and nutritional quality of packed items by reducing microbial load and oxidative spoilage (Vermeiren *et al*. 1999; Kumar *et al*. 2018). However, stabilization problems occur due to the high volatility of essential oils and their limited tendency to distribute homogeneously within the film matrix. Therefore, special techniques such as encapsulation and emulsification are applied to integrate the essential oil into the matrix (Stoleru and Brebu 2021).

In this study, clove (*Syzygium aromaticum*) essential oil was used to provide active protection to HPMC/CaLS packaging films. The main component of clove essential oil,

eugenol, is classified by the World Health Organization (WHO) as a substance generally recognized as safe (GRAS) and is noted for its powerful antibacterial, antioxidant, anti-inflammatory, and antiseptic properties (Silva *et al*. 2024). Thanks to this, it finds a wide range of applications in the cosmetics, food, and pharmaceutical industries (Zare *et al*. 2026). The film was prepared in an aqueous medium because HPMC and CaLS are water-soluble and this approach avoids toxic contamination. However, since the neat essential oil is not soluble in water, it was incorporated into the film using an intermediate phase. To ensure homogeneous integration of the essential oil into the matrix, the emulsion method using Polyoxyl-40 Castor Oil was chosen.

Although the individual use of cellulose and lignin derivatives in packaging films has been extensively studied in the literature, there are only a limited number of studies on film systems in which these two components are enriched with an essential oil emulsion. In this context, the present study aimed to develop multifunctional green packaging films that possess both UV-blocking and antibacterial properties by combining the cellulose derivative HPMC with calcium lignosulfonate, an industrial lignocellulosic byproduct. The study systematically investigated how the properties of the active packaging changed when clove essential oil was incorporated into this base matrix at different concentrations. Moreover, it also offers a comprehensive perspective on the utilization of various fractions of forest biomass -ranging from structural polymers to aromatic secondary metabolites- for industrial applications and is expected to contribute to the development of sustainable packaging technologies.

EXPERIMENTAL

Materials

Plant-base HPMC (~86 kDa) was used as the base polymer and purchased from Sigma Aldrich, USA. CaLS powder (84% lignin, %16 ash) was supplied from DMR Chemistry Company, Türkiye. Clove (*Syzygium aromaticum*) buds originated Indonesia were purchased from a local supplier and plant identification was provided by Bursa Technical University Faculty of Forestry. Polyoxyl-40 Castor Oil was used as a non-ionic emulsifying agent and purchased from Merck, Germany.

Extraction of Essential Oil

The essential oil was obtained using microwave assisted extraction technology (Neos Milestone, Italy). 1 L of distilled water was added to 500 g of clove buds. The power/time parameters were set to 700 W for 20 min, and then to 500 W for 30 min. The obtained oil was stored at -18 °C in a sealed vial. The yield of the essential oil was calculated according to Eq. 1,

$$\text{Yield (\%)} = (W_{eo} / M) \times 100 \quad (1)$$

where W_{eo} represents the volume of the essential oil obtained (mL), and M represents the weight (g) of the clove buds used.

Gas Chromatography (GC)- Mass Spectroscopy (MS) Analysis

GC-MS analysis of essential oil was performed after dilution with n-hexane at a ratio of 1/20 (v/v) employing an Agilent GC-MS device equipped with a HP-5MS (30m x 0.250 mm x 0.25 μm) column. The analysis was performed using helium as the carrier gas,

with a flow rate of 1 mL/min and a split ratio of 1/5. The inlet temperature was set to 250 °C and the injection volume to 1 µL. The temperature program started at 60 °C and increasing to 300 °C at a rate of 3 °C/min (Ertaş *et al*. 2019). A library search performed against the NIST17 spectral database aided in the identification of chemical compounds (Öz *et al*. 2026).

Preparation of Active Films

The films were prepared using the solution casting technique according to the ratios specified in Table 1. The production stages are summarized in Fig. 1. The clove essential oil emulsion (SAEO) was prepared separately prior to film preparation. The emulsion has been formulated with a volume ratio of 1:1:8 for essential oil, Polyoxyl-40, and water. The pre-emulsion was prepared by vortexing the components for 5 min at room temperature. Subsequently, the emulsion was sonicated in an ultrasonic bath for 10 min to achieve greater homogeneity. The prepared emulsion was added fresh to the film-forming solution.

Table 1. Preparation of Active Packaging Films

Sample ID	HPMC (wt.%)	CaLS (wt.%)	SAEO (wt.%)
HPMC	100	-	-
HPMC/CaLS	90	10	-
APF/2	88	10	2
APF/4	86	10	4
APF/6	84	10	6

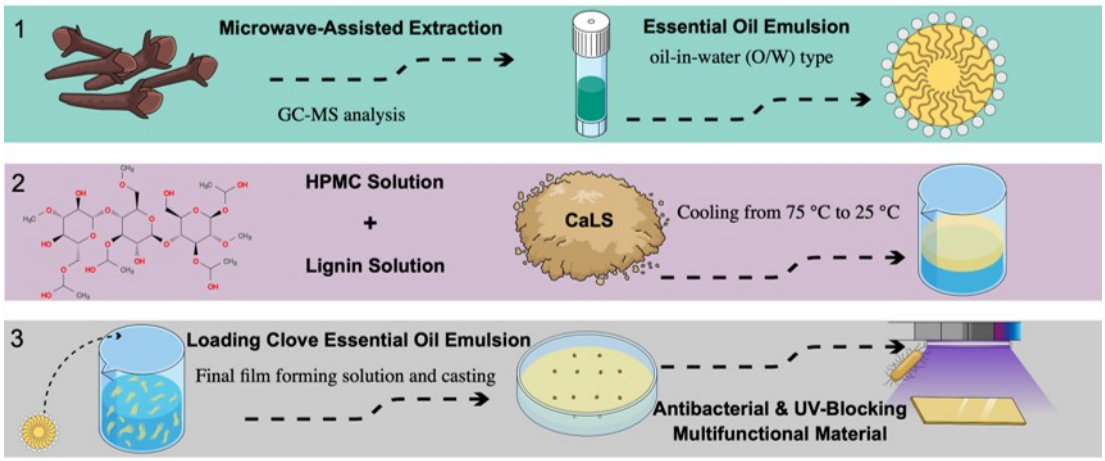

Fig. 1. Essential oil emulsion preparation and film making procedures

The film forming solution was prepared by stirring HPMC in 95 mL distilled water at 75 °C for 1 h. A CaLS solution prepared with 5 mL of distilled water was added, and the heater was turned off. Once the solution cooled to room temperature, SAEO was added. No external heat was applied during film drying to prevent possible losses of volatile essential oil components due to increased temperature. Additionally, the drying process was limited to 24 hours because rapid or excessive drying may lead to cracking and pore formation in the film structure. The final solution was dried at room temperature in an acrylic petri dish (d:14 cm).

Fourier Transform Infrared Spectroscopy (FTIR) Analysis

Attenuated total reflection (ATR)-FTIR measurements of films were performed with a Bruker Tensor branded device. FTIR spectra were recorded at wavelengths ranging from 400 to 4000 cm^{-1}. The measurements were performed at a spectral resolution of 4 cm^{-1} with 32 scans.

Thermogravimetric Analysis (TGA)

Hitachi STA7200 brand thermal analyzer was used for thermal measurements. The analysis was performed by heating the samples from 30 °C to 800 °C at a rate of 10 °C/min under inert atmosphere (nitrogene) flowing at 200 mL/min.

Color Measurement

The color of films was assessed according to the CIE-L*a*b* color scale using the Konica-Minolta 2600D device. The color differences (ΔE) of films were calculated with Eq. 2,

$$\Delta E = \sqrt{(L_1^* - L_2^*)^2 + (a_1^* - a_2^*)^2 + (b_1^* - b_2^*)^2} \quad (2)$$

where L_2*, a_2*, and b_2* were the color values of reference white base (L* = 91.48, a* = 2.59, b* = 10.65), and L_1*, a_1*, and b_1* were the color parameters of films.

Mechanical Analysis

The thickness of each test specimen was analyzed in five areas employing a Mitutoyo micrometer. The Testform/AS3 universal test machine was used in the analysis of the tensile strength (TS) and elongation at break (EAB) of the specimen under the load of 1 kN based on ASTM D882 (2018).

Scanning Electron Microscopy (SEM)

The surface features of the films were captured using a Carl Zeiss/Gemini 300 (Germany). Films were coated with 15 nm of gold to avoid charging effects before analysis.

UV-Blocking and Opacity Measurement

The UV-blocking properties and opacity of the film samples were determined using a UV-Vis spectrophotometer (Hach Lange Dr 3900, USA). UV-blocking percentage was assessed based on the film's transmittance at 280 nm (Eq. 3) based on Lambert-Beer's Law (Oladzadabbasabadi *et al*. 2026).

$$\text{UV-Blocking Performance (\%)} = 100 - \%T_{280} \quad (3)$$

Opacity was calculated using the film's absorbance at 600 nm (Eq. 4). This measurement serves as a preliminary evaluation of the film's suitability for light-sensitive packaging applications,

$$\text{Opacity} = A_{600} / t_{\text{sample}} \quad (4)$$

where A represents the absorbance value, and t represents the average thickness (mm) of the sample.

Antibacterial Analysis

The antibacterial activity of the films was evaluated using a slightly modified ASTM E2149-13a (2020) standard, a quantitative antimicrobial test method performed under dynamic-contact conditions (Di Matteo *et al*. 2026). Gram-negative *Escherichia coli* ATCC 25922 and Gram-positive *Staphylococcus aureus* ATCC 25923 were firstly cultured on Nutrient Agar (NA) at 37 °C for 24 h. A single colony was then transferred into Nutrient Broth (NB) and incubated under the same conditions to create a fresh bacterial suspension. The cultures were subsequently diluted with NB to obtain a final working concentration of 1.8×10^5 CFU/mL. Before the analysis, films were sterilized under UV-C light for 30 min on each side to remove surface contamination. Then, 0.5 g of each sample was aseptically transferred into sterile conical flasks containing 50 mL of bacterial suspension. The flasks were incubated at 37 °C with shaking at 110 rpm for 24 h to provide continuous contact between the bacteria and the sample. After incubation period, aliquots were taken from each flask and subjected to serial dilution using sterile saline solution. Appropriate dilutions were plated on NA and incubated at 37 °C for 24 h. The number of viable bacteria was determined by counting colony-forming units (CFU), and the results were expressed as CFU/mL. The antibacterial activity was evaluated by comparing the bacterial counts of the samples with the untreated bacterial control. The percentage of bacterial reduction (R%) was calculated using Eq. 5,

$$R\%\left(\frac{CFU}{mL}\right) = \left[\frac{B-A}{B}\right] x\ 100 \quad (5)$$

where A and B represent the number of viable bacteria recovered from the treated samples and untreated control after 24 h, respectively.

$$Log_{10}\ bacteria\ reduction = Log_{10}(B) - Log_{10}(A) \quad (6)$$

RESULTS AND DISCUSSION

Yield and Chemical Profile of Essential Oil

The yield of clove essential oil was determined to be 13.7% ± 0.4 on a dry weight basis. A previous study examining clove buds collected from nearby regions indicated that the essential oil content may range from 12% to 20%, aligning with the results of the current investigation (Susilowati *et al*. 2025). According to the GC-MS report (Table 2), the most abundant component in clove essential oil was identified as eugenol (86.9%) consistent with literature (Alma *et al*. 2007).

Table 2. GC-MS Report of Clove Essential Oil

Retention time (min)	Component name	Area (%)	RI[a*]	RI[b*]
20.87	Eugenol	86.86	1379	1356
21.55	α-Copaene	0.25	1387	1374
23.32	β-Caryophyllene	11.27	1409	1417
24.69	α-Humulene	1.44	1426	1432
27.51	Δ-Cadinene	0.18	1462	1513
* RI[a]: Retention index calculated RI[b]: Retention index from literature				

Additionally, some studies have reported the presence of lower amount of eugenol, but these studies also found its derivative forms such as eugenol acetate (Kaur *et al*. 2019;

Tarhan 2021). The eugenol-dominant chemical profile of the oil may be advantageous for antimicrobial applications, considering that eugenol is the primary bioactive compound responsible for microbial inhibition (Marchese *et al*. 2017).

While essential oils have been widely investigated, their complex chemical composition often makes it difficult to attribute the observed activity to specific components. Most essential oils consist of numerous compounds in varying proportions, leading to potential synergistic or antagonistic effects (Martucci *et al*. 2015). The essential oil selected in this study has a relatively simple composition, as evidenced by GC-MS analysis. This approach offers an advantage over multi-component essential oils, as it reduces compositional complexity and allows for a more controlled interpretation of functional properties. In support of this, a combined evaluation of both eugenol and eugenol-containing essential oils has shown that the major antimicrobial effect originates from eugenol (Marchese *et al*. 2017).

FTIR Analysis

The FTIR spectra of the materials are shown in Fig. 2. The broad peak observed at 3432 cm^{-1} in the FTIR spectrum of HPMC represents hydroxyl (-OH) groups. The peak at 2887 cm^{-1} corresponds to the C-H stretch and can be attributed to the presence of methyl and hydroxypropyl groups in the HPMC structure. The sharp peak occurring at 1055 cm^{-1} represents the glycosidic bonds in the cellulose ring and the ether (C-O-C) groups in the side chains (Aydogdu *et al*. 2018).

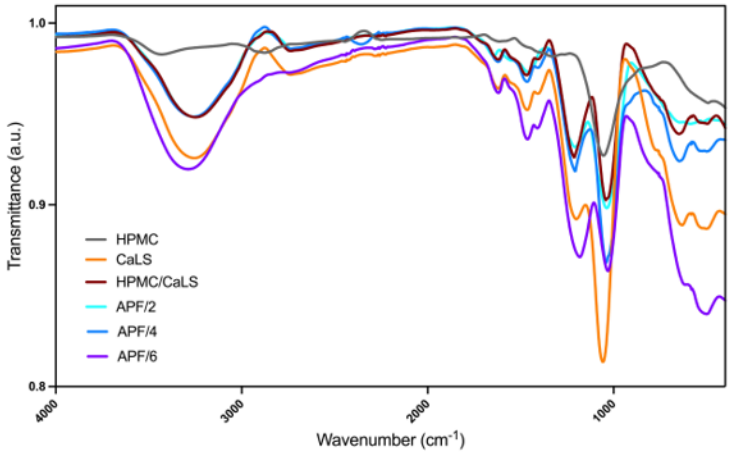

Fig. 2. FTIR spectra of raw materials and CaLS/SAEO-incorporated film samples

The peak observed at a wavenumber of 3250 cm^{-1} in the CaLS spectrum was attributed to the stretching vibrations of the phenolic hydroxyl (-OH) groups, which are abundant in the lignin structure. The peaks observed between 1615 and 1518 cm^{-1} are characteristic of CaLS. These peaks originate from the vibrations of the phenylpropane units that build the lignin structure, and they are believed to represent C=C stretching vibrations of the aromatic ring. The signals at approximately 1248 and 1072 cm^{-1} correspond to the asymmetric and symmetric vibrations of the sulfonate groups (S=O), respectively (Zhang *et al*. 2025). The FTIR spectra of samples containing essential oils were similar to each other. The methoxy group (-OCH_3) in the structure of eugenol, the major component of clove essential oil, increased the peak intensity around 1200 to 1210 cm^{-1}.

TGA Measurement

The thermal behavior of the films was investigated by TGA (Fig. 3). The initial degradation was observed from 50 to 98 °C. This behavior is attributed to the removal of free and bound water present in the samples. A remarkable mass loss was observed in this region, particularly in samples containing CaLS. This is likely due to the hydrophilic nature of sulfonate ($-SO_3^-$) and hydroxyl (-OH) groups in the structure of lignosulfonate hold water molecules within the matrix through hydrogen bonds (Tang *et al*. 2023). The small peaks observed between 143 to 187 °C on the DTG curve of the SAEO-containing groups are due to the degradation of the volatile essential oil components (predominantly eugenol) in the emulsion. Supporting this, the most pronounced peak in this range was observed in the APF6 sample, which contained the highest percentage (6%) of SAEO. It should also be noted that the films were dried at room temperature rather than by elevated-temperature drying; the mild condition was deliberately chosen to minimize thermally driven volatilization of the essential oil during film formation. The relatively high boiling point of eugenol (~254 °C) and its incorporation as an emulsion entrapped within the HPMC matrix further favor its retention by limiting diffusion to the film surface and evaporation (Stoleru and Brebu 2021). The persistence of the DTG mass-loss peak at 143 to 187 °C in the films confirms that a measurable fraction of eugenol was retained after drying. Nevertheless, gradual evaporative loss during prolonged storage remains an inherent limitation of such films, and quantitative retention/release tracking together with further encapsulation strategies is proposed as future work. The main thermal degradation of the films occurred starting with HPMC at 364.9 °C and continuing with CaLS at 390.8 °C. The major degradation temperature of films containing 2 wt.% and 4wt.% SAEO (APF2 and APF4) was found to be approximately 10 °C higher than neat HPMC, despite the presence of thermally unstable Polyoxyl-40 content in the emulsion. This is because HPMC has a more linear structure, and the glycosidic bonds of cellulose are more easily broken under thermal effects. In contrast, CaLS has a more complex and partially cross-linked structure containing aromatic rings; therefore, lignin-blended materials generally exhibit greater resistance to thermal degradation (Zor *et al*. 2023).

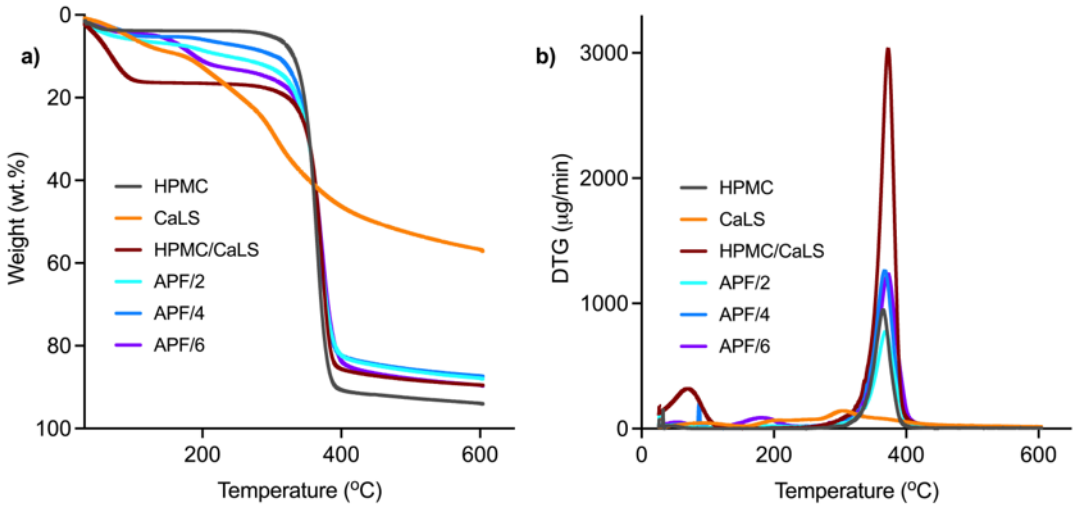

Fig. 3. a) TG and b) DTG curves of raw materials and CaLS/SAEO-incorporated film samples

The maximum degradation temperature APF6 (containing 6% SAEO) decreased slightly compared to neat HPMC. This behavior may be attributed to possible phase separation and microstructural heterogeneity at higher oil loadings, which may lead to reduced structural integrity and thereby accelerate thermal decomposition (Stramarkou *et al*. 2020). When the residue amounts of the samples at 600 °C were examined, the residue amount increased by approximately two times with the addition of CaLS compared to pure HPMC. This can be attributed to the fact that CaLS has a heat-resistant character and promotes carbonization (char) formation and leaving a higher residue (Cavdar *et al*. 2025).

Color Measurement

The color axes of the films were evaluated in the CIELab (L^*, a^*, b^*) color space, and the results are given in Table 3. The pure HPMC sample was determined to be the lightest colored sample with the highest L^* value (97.9). In the HPMC/CaLS sample containing lignosulfonate, a significant decrease in the L^* value (77.7) was observed, indicating a noticeable darkening of the film. This darkening is thought to be due to the aromatic structure and naturally dark character of lignosulfonate. Adding SAEO to the films resulted in a slight lightening of the color because essential oil emulsions have a characteristic milky white color.

Table 3. Color Measurements of Samples

Sample ID	L^*	a^*	b^*	ΔE
HPMC	97.93 (3.41)^{a}	-0.35 (0.06)^{a}	1.17 (0.34)^{a}	1.45 (0.30)^{a}
HPMC/CaLS	77.70 (4.20)^{d}	1.06 (1.14)^{b}	31.62 (3.67)^{c}	31.88 (3.75)^{c,d}
APF/2	84.18 (2.94)^{b}	0.74 (0.66)^{b}	27.65 (3.23)^{b}	27.98 (3.35)^{b}
APF/4	82.18 (5.11)^{c}	1.32 (1.05)^{b}	34.80 (3.98)^{d}	35.12 (4.10)^{d}
APF/6	84.05 (3.72)^{b}	1.68 (1.20)^{b}	30.83 (6.27)^{c}	31.10 (6.45)^{c}

Values are expressed as mean ± standard deviation (shown in parentheses). Different lowercase letters within each column indicate significant differences between samples ($p < 0.05$; n=5).

The most remarkable color change occurred along the b^* axis. The b^* value, which was 1.17 in the neat HPMC sample, increased to over 30 with the addition of CaLS and SAEO, showing the formation of yellow-brown tones in the films. This change indicates that both the chromophore groups in the lignosulfonate structure and the essential oil components contributed holistically to UV-blocking performance and color formation. When the total color difference (ΔE) values were examined, it was determined that neat HPMC film was close to the reference value ($\Delta E < 2$), and the APF4 sample showed the most pronounced color change with the highest ΔE value. From a marketing perspective, the color of the packaging should also be taken into consideration. Although Kozik-Kołodziej *et al.* (2026) reported that consumers are generally willing to pay a premium of approximately 20% for bio-based packaging, Ningtyas *et al.* (2025) noted that the brown color of lignin may influence consumers' purchasing decisions, since transparency and visual appearance remain important factors in food packaging.

Mechanical Analysis

The thickness and mechanical properties of films are represented in Table 4. The addition of CaLS to the HPMC matrix resulted in an approximately 9% increase in the TS value compared to a neat HPMC film. Similar results have been observed in previous studies and have been attributed to the strong hydrogen bonds and electrostatic interactions

formed between the sulfonate and hydroxyl groups in CaLS and the hydroxyl groups of the base polymer (Ye *et al*. 2016; Liu *et al*. 2023). The addition of CaLS reduced the EaB value from 15.0% to 12.4%. This decrease is attributed to the increased crosslinking network restricting the mobility of the polymer chains and the matrix acquiring a stiffer but less flexible structure. A concentration-dependent decrease in TS values was observed with the addition of SAEO. This reduction is attributed to oil droplets dispersed throughout the film matrix weakening the interactions between polymer chains and thereby disrupting the homogeneity of the film structure (Rui *et al*. 2024). The EaB values increased with the addition of the SAEO, reaching 17.01% in APF2, while they remained at approximately 16% in the APF4 and APF6 samples. This behavior is explained by the secondary plasticizing effect of Polyoxyl-40, which was used as an emulsifier (Brandelero *et al*. 2012). Consequently, the addition of CaLS enhanced the strength while reducing flexibility, whereas the SAEO partially recovered the EaB capacity without significantly affecting the TS. This balanced profile is particularly evident in the APF2 and APF4 films, which exhibit a steady profile in terms of mechanical strength and flexibility.

Table 4. Mechanical Test Results of Film Samples

Sample ID	Thickness (mm)	TS (MPa)	EaB (%)
HPMC	0.082 (0.011)[a]	45.05 (0.06)[a]	15.03 (1.08)[a]
HPMC/CaLS	0.089 (0.008)[b]	49.06 (2.31)[b]	12.45 (2.01)[b]
APF/2	0.106 (0.022)[c]	46.94 (1.96)[c]	17.01(3.13)[c]
APF/4	0.133 (0.034)[d]	44.93 (1.43)[a]	16.22 (1.56)[d]
APF/6	0.125 (0.057)[e]	41.64 (2.20)[d]	16.01 (1.78)[d]
Values are expressed as mean ± standard deviation (shown in parentheses). Different lowercase letters within each column indicate significant differences between samples ($p < 0.05$; n=5)			

Morphological Properties

SEM images of the film samples are shown in Fig. 4.

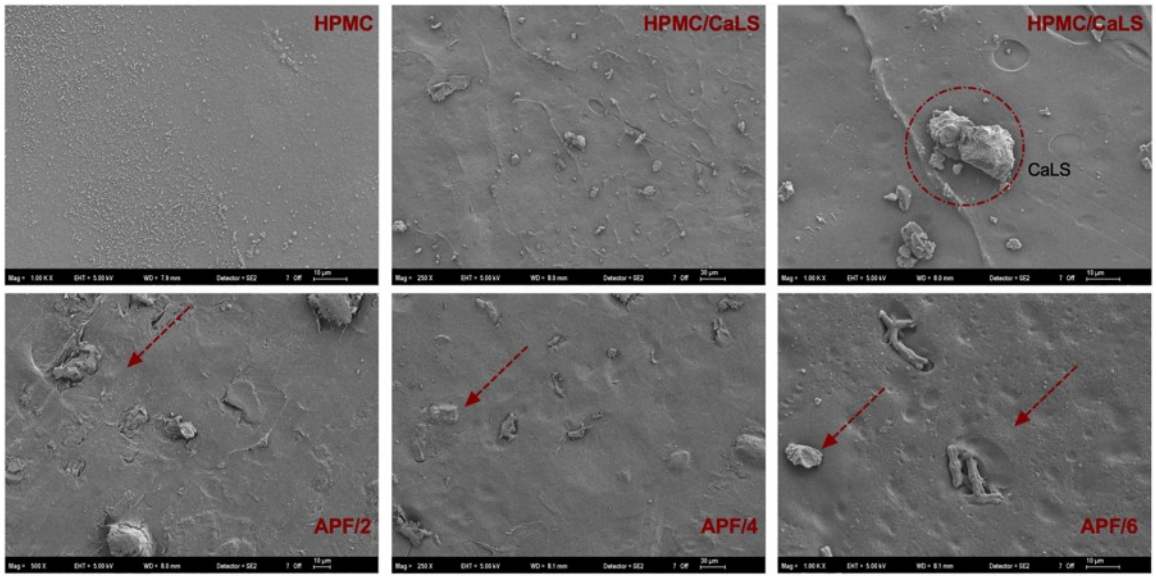

Fig. 4. SEM images of neat HPMC and CaLS/SAEO-incorporated film samples

The minor particle structures observed on the surface of neat HPMC result from agglomeration occurring during the drying process, and a homogeneous film formation was observed in accordance with the literature (Perone *et al*. 2014). In the HPMC/CaLS sample, crystalline CaLS particles were observed on the surface. While the film dries, water evaporates, and CaLS molecules can aggregate to form regular salt crystal-like structures. Furthermore, the sulfonate ($-SO_3^-$) groups in CaLS are highly hydrophilic and tend to hold water within their structure during drying. As a result, local concentration differences could arise, leading to localized aggregation points on the surface (Roy *et al*. 2024).

In APF/2 and APF/4 films, it was observed that CaLS particles were embedded in the matrix and that overall surface homogeneity improved compared to the HPMC/CaLS film. This may indicate that the Polyoxyl-40 not only emulsified the essential oil but also played a secondary role in creating a more homogeneous dispersion medium by reducing the surface tension of the CaLS particles within the film (Liang *et al*. 2025). The APF/6 film exhibited quite heterogeneity characterized by crater-like structures distributed across the surface. This is attributed to the excessive SAEO content surpassing the matrix's capacity to retain homogeneous dispersion and leading to phase separation during the film forming. A similar change has also been reported in HPMC-based composite films as the additive concentration was increased (De Farias *et al*. 2025). The heterogeneity of APF/6 is also consistent with its relatively poor results of the mechanical tests (Mafe *et al*. 2025).

UV-Blocking Properties

The UV-blocking ratios of the films are shown in Fig. 5a. The neat HPMC film has a UV-blocking capacity of approximately 55%. Adding CaLS to the matrix significantly increased this value to as high as 98%. This behavior is attributed to the superior UV absorption properties of lignin, which originated from the chromophore groups in its aromatic structure (Ruwoldt *et al*. 2023; Laleicke and Hubbe 2025). In previous research, the UV blocking percentage of chitosan/sodium lignosulfonate films reached 95% (Liu *et al*. 2023). Thus, the findings of the study were consistent with the literature.

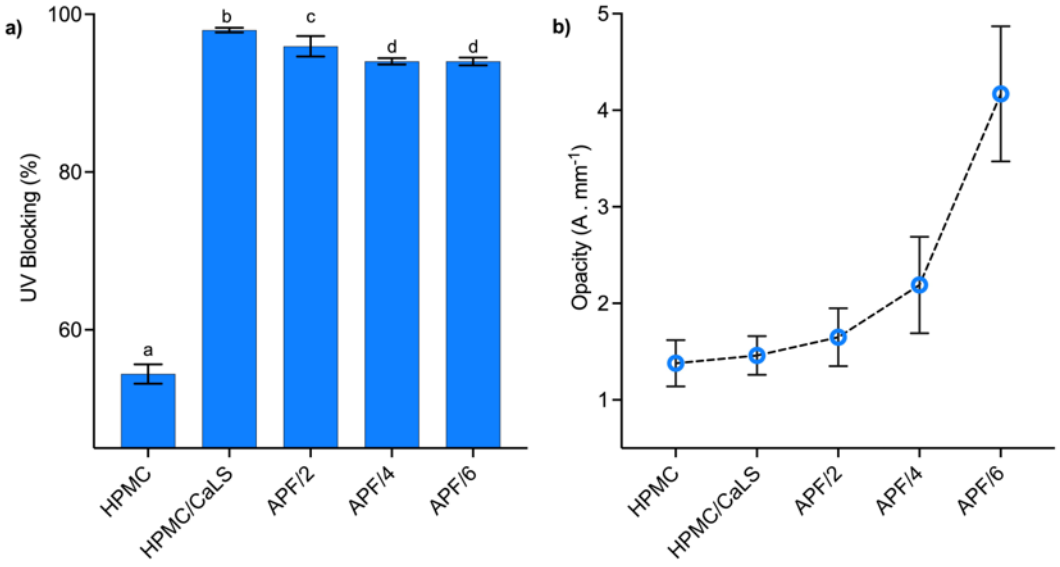

Fig. 5. a) UV-Blocking performance and b) opacity of film samples

The UV blocking rates of films containing SAEO (APF2, APF4, and APF6) were measured at 95%, 94%, and 94%, respectively. These slight decreases may be due to emulsified oil droplets that partially disrupt the homogeneity of the film matrix, or to the diluting effect of Polyoxyl-40 in the matrix. The essential oil itself was not assessed to have a direct effect on UV properties (Jahromi *et al*. 2022). Adding clove essential oil at concentrations of 1% and 5% to Pullulan/PET/PP films did not result in a significant change in UV transmittance (Kraśniewska and Gniewosz 2025).

Opacity is one of the key parameters that determine barrier performance in packaging applications. High opacity values can slow down photooxidation by reducing light transmission, thereby extending the shelf life of products with high oil content or sensitive to light (Lu and Xu 2009; Tripathi *et al*. 2024). The opacity of neat HPMC was measured at approximately 1.17 $A.mm^{-1}$, and the value increased to 4.17 $A.mm^{-1}$ with the incorporation of additives (Fig. 5b). The increase in opacity values in films containing SAEO can be ascribed to the light scattering caused by emulsion droplets. The standard deviations of the samples containing SAEO also increased. This can be attributed to variations in droplet size and the potential for heterogeneity in films with higher essential oil content (APF/4 and APF/6).

Antibacterial Activity of Films

The antibacterial activity of the films was evaluated against *E. coli* and *S. aureus* under dynamic contact conditions. The initial bacterial concentration used in the assay was approximately 1.8×10^5 CFU/mL for both strains. After 24 h, the untreated control reached 6.6×10^8 CFU/mL for *E. coli* and 5.4×10^8 CFU/mL for *S. aureus*. Comparing neat HPMC and HPMC/CaLS film, it was observed that the addition of CaLS alone did not produce a significant antibacterial effect (Fig. 6a).

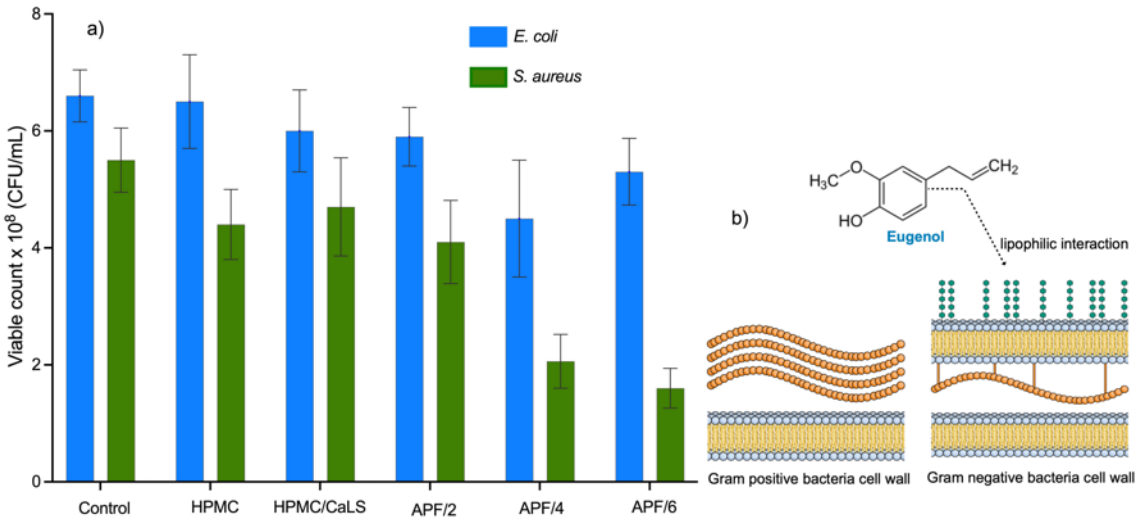

Fig. 6. a) antibacterial performance of film samples b) bacteria cell wall structure

Although lignin can exhibit antimicrobial properties due to its polyphenolic structure and oxygen-containing functional groups, it has been reported that this activity varies significantly depending on the type of lignin, the biomass source, and the processing method (pulping) applied (Alzagameem *et al*. 2019). This finding indicates that a 10% CaLS addition did not act as a direct antibacterial agent and the primary active antibacterial component in the formulation was clove essential oil. It was determined that antibacterial

activity increased with concentration in formulations containing clove essential oil. Notably, the film containing 6 wt.% SAEO (APF6) achieved an approximate 99% reduction against *E. coli* and around 70 wt.% against *S. aureus* (Fig. 4a). These findings align with previous studies indicating that clove oil formulations can result in reductions of up to 5 logs, with *E. coli* generally being more susceptible than *S. aureus* (Nuñez and D'Aquino 2012).

When compared to these findings, the antibacterial performance evaluated under ASTM E2149-13a (2020) conditions showed a more noticeable effect, especially against *E. coli*. The reduced susceptibility of *S. aureus* aligns with existing literature and can be attributed to differences in cell wall structure (Sayed *et al*. 2023). This antibacterial effect is primarily linked to eugenol, which disrupts bacterial membranes and increases permeability, ultimately resulting in cell death. Due to its lipophilic nature, eugenol interacts effectively with lipid-rich membranes, which may enhance its activity against Gram-negative bacteria (Fig. 6b).

Table 5. The Antibacterial Activity of the Films

Bacteria	Sample	Log reduction	% Reduction
E. coli	Bacteria control	-	-
	HPMC	0.01	1.52
	HPMC/CaLS	0.04	9.09
	APF2	0.05	10.61
	APF4	0.17	31.82
	APF6	2.10	99.20
S. aureus	Bacteria control	-	-
	HPMC	0.09	18.52
	HPMC/CaLS	0.06	12.96
	APF2	0.12	24.07
	APF4	0.42	61.85
	APF6	0.53	70.37

Although Gram-negative bacteria are generally considered more resistant to essential oils because of their lipopolysaccharide-containing outer membrane, the clove essential oil used in the present study exhibited greater antibacterial activity against *E. coli* than against *S. aureus*. This difference can be explained in greater detail by examining the cellular structure of the two bacteria (Gill and Holley 2006). Although the outer membrane of *E. coli*, which contains lipopolysaccharides, initially forms a protective barrier against hydrophobic compounds, eugenol can increase its permeability by disrupting the lipid arrangement of this membrane (Marchese *et al*. 2017). In contrast, even though *S. aureus* does not have an outer membrane, its cell wall containing a thicker peptidoglycan layer and teichoic acid may have delayed the penetration of eugenol released from the HPMC matrix into the cytoplasmic membrane or reduced its effectiveness. Therefore, the higher antibacterial activity of the APF6 film against *E. coli* should be considered not only in terms of Gram classification but also in relation to eugenol's interaction with the cell membrane, its release behavior from the film, and the strain-specific susceptibilities of the bacteria.

CONCLUSIONS

1. According to gas chromatography-mass spectrometry (GC-MS) analysis, eugenol was determined as main component of the clove essential oil (86.9%), and the relatively simple chemical profile of the oil may be allowed for a more controlled interpretation of the observed antimicrobial properties compared to complex essential oils.
2. Calcium lignosulfonate (CaLS) remarkably improved the UV-blocking capacity of the neat HPMC film, increasing it from approximately 55% to 98%. This phenomenon is attributed to the existence of UV-absorbing groups (chromophore) in the aromatic structure of lignin. Upon incorporation of *Syzygium aromaticum* essential oil (SAEO), UV-blocking performance decreased slightly to 94-95%, which was likely due to partial disruption of matrix homogeneity due to emulsified oil droplets.
3. The addition of CaLS to the hydroxypropylmethylcellulose (HPMC) matrix resulted in an approximately 9% increase in tensile strength. SAEO incorporation reduced tensile strength while partially recovering elongation at break and it may associate with the plasticizing properties of Polyoxyl-40. The APF2 and APF4 films achieved a balanced mechanical profile suitable for flexible packaging applications.
4. Clove essential oil was the primary ingredient responsible for bacterial inhibition, and it was observed that CaLS addition alone exhibited no inhibition. Antibacterial activity increased with SAEO concentration, specifically samples containing 6 wt.% SAEO achieved approximately 99% reduction against *Escherichia coli* and 70% against *Staphylococcus aureus*.

ACKNOWLEDGMENTS

The author would like to express her gratitude to K. Bezir and M.M. Cagal for their support during the antibacterial analysis.

Conflict of Interest

The author declares no conflict of interest.

Use of Generative AI

This manuscript was partially checked for language and grammar issues using Gemini AI.

REFERENCES CITED

Alma, M. H., Ertaş, M., Nitz, S., and Kollmannsberger, H. (2007). "Chemical composition and content of essential oil from the bud of cultivated Turkish clove (*Syzygium aromaticum* L.)," *BioResources* 2(2), 265-269. https://doi.org/10.15376/biores.2.2.265-269

Alzagameem, A., Klein, S. E., Bergs, M., Do, X. T., Korte, I., Dohlen, S., Hüwe, C., Kreyenschmidt, J., Kamm, B., Larkins, M., and Schulze, M. (2019). "Antimicrobial activity of lignin and lignin-derived cellulose and chitosan composites against selected pathogenic and spoilage microorganisms," *Polymers* 11(4), article 670.

https://doi.org/10.3390/polym11040670
ASTM D882-12 (2018). "Standard test method for tensile properties of thin plastic sheeting," ASTM International, West Conshohocken, PA, USA.
ASTM E2149-13a (2020). "Standard test method for determining the antimicrobial activity of antimicrobial agents under dynamic contact conditions," ASTM International, West Conshohocken, PA, USA.
Atarés, L., and Chiralt, A. (2016). "Essential oils as additives in biodegradable films and coatings for active food packaging," *Trends in Food Science & Technology* 48, 51-62. https://doi.org/10.1016/j.tifs.2015.12.001
Aydogdu, A., Sumnu, G., and Sahin, S. (2018). "A novel electrospun hydroxypropyl methylcellulose/polyethylene oxide blend nanofibers: Morphology and physicochemical properties," *Carbohydrate Polymers* 181, 234-246. https://doi.org/10.1016/j.carbpol.2017.10.071
Brandelero, R. P. H., Grossmann, M. V. E., and Yamashita, F. (2012). "Films of starch and poly (butylene adipate co-terephthalate) added of soybean oil (SO) and Tween 80," *Carbohydrate Polymers* 90(4), 1452-1460. https://doi.org/10.1016/j.carbpol.2012.07.015
Cavdar, A. D., Torun, S. B., and Mengeloglu, F. (2025). "The engineering properties of polypropylene hybrid composites reinforced with lignin and zeolite," *Journal of Materials Research and Technology* 38, 2666-2674. https://doi.org/10.1016/j.jmrt.2025.08.100
Erişir, E., and Gümüşkaya, E. (2024). "Acetylation of cellulose in ethyl acetate: Characterization and thin film applications," *Journal of Wood Chemistry and Technology* 44(4), 228-243. https://doi.org/10.1080/02773813.2024.2365142
Ertaş, M., Fidan, M. S., Kaya, S., and Angın, N. (2019). "Kara Ardıç (Juniperus sabina L.) kozalaklarından elde edilen uçucu yağın kimyasal bileşimi üzerine mikrodalga ve hidrodestilasyon yöntemlerinin etkisi," *Artvin Çoruh Üniversitesi Orman Fakültesi Dergisi* 20(2), 272-277.
De Farias, P. M., De Sousa, R. V., Maniglia, B. C., Pascall, M., Matthes, J., Sadzik, A., Schmid, M., and Fai, A. E. C. (2025). "Biobased food packaging systems functionalized with essential oil via Pickering emulsion: Advantages, challenges, and current applications," *ACS Omega* 10(5), 4173-4186. https://doi.org/10.1021/acsomega.4c09320
Gill, A. O., and Holley, R. A. (2006). "Disruption of *Escherichia coli*, *Listeria monocytogenes* and *Lactobacillus sakei* cellular membranes by plant oil aromatics," *International Journal of Food Microbiology* 108(1), 1-9. https://doi.org/10.1016/j.ijfoodmicro.2005.10.009
Guo, J., Rawdkuen, S., Zhang, W., Kingwascharapong, P., and Xia, G. (2025). "Research progress of biopolymer-based food packaging films/coatings functionalized with edible photosensitizers," *Trends in Food Science & Technology* 162, 105078. https://doi.org/10.1016/j.tifs.2025.105078
Guo, Y., You, Y., Guo, G., Chen, Z., Peng, W., Hu, L., Liang, S., and Xie, H. (2023). "Facile preparation of cellulose/lignosulfonate derivatives composite films with high UV-shielding and gas barrier properties," *International Journal of Biological Macromolecules* 237, article 124218. https://doi.org/10.1016/j.ijbiomac.2023.124218
Jahromi, M., Niakousari, M., and Golmakani, M. T. (2022). "Fabrication and characterization of pectin films incorporated with clove essential oil emulsions

stabilized by modified sodium caseinate," *Food Packaging and Shelf Life* 32, article 100835. https://doi.org/10.1016/j.fpsl.2022.100835

Jha, A., and Kumar, A. (2025). "Sodium lignosulfonate inhibits multiple virulent proteins of human fungal pathogen *Candida albicans*," *Archives of Microbiology* 207(1), 8. https://doi.org/10.1007/s00203-024-04201-2

Kaur, K., Kaushal, S., and Rani, R. (2019). "Chemical composition, antioxidant and antifungal potential of clove (*Syzygium aromaticum*) essential oil, its major compound and its derivatives," *Journal of Essential Oil Bearing Plants* 22(5), 1195-1217. https://doi.org/10.1080/0972060X.2019.1688689

Kozik-Kołodziej, N. (2026). "Consumer attitudes and perceptions toward sustainable packaging: A systematic literature review," *Sustainability* 18(3), article 1235. https://doi.org/10.3390/su18031235

Kraśniewska, K., and Gniewosz, M. (2025). "Active packaging based on a PET/PP food-grade film coated with pullulan and clove essential oil: Physicochemical and antimicrobial properties," *Molecules* 30(10), article 2118. https://doi.org/10.3390/molecules30102118

Kumar, K. V. P., Suneetha, J., and Kumari, B. A. (2018). "Active packaging systems in food packaging for enhanced shelf life," *Journal of Pharmacognosy and Phytochemistry* 7, 2044-2046.

Laleicke, P. F., and Hubbe, M. A. (2025). "Outdoor wood finishing: A review on making wood resistant to moisture, ultraviolet light, and degradation," *BioResources* 20(3). 7903-7982. https://doi.org/10.15376/biores.20.3.Laleicke

Liang, X., Duan, X., Du, Y., Tang, Z., Ma, Z., Zhu, N., Yang, A., and Tang, Y. (2025). "Combining porous starch and polyoxyethylene hydrogenated castor oil RH40 to enhance the solubility, stability, and bioavailability of bisdemethoxycurcumin," *International Journal of Biological Macromolecules* 309, article 143189. https://doi.org/10.1016/j.ijbiomac.2025.143189

Liu, X., Chen, C., Cao, Y., Peng, C., Fang, J., Wang, H., Wu, W., Lyu, G., and Li, H. (2023). "Effect and enhancement mechanism of sodium lignosulfonate on the chitosan-based composite film," *Colloids and Surfaces A: Physicochemical and Engineering Aspects* 678, article 132505. https://doi.org/10.1016/j.colsurfa.2023.132505

Lu, L., and Xu, F. (2009). "Effect of light-barrier property of packaging film on the photo-oxidation and shelf life of cookies based on accelerated tests," *Packaging Technology and Science* 22(2), 107-113. https://doi.org/10.1002/pts.838

Mafe, A. N., Edo, G. I., Ali, A. B. M., Akpoghelie, P. O., Yousif, E., Isoje, E. F., Igbuku, U. A., Opiti, R. A., Ajiduku, L. A., and Owheruo, J. O. (2025). "Next-generation biopolymers for sustainable food packaging: Innovations in material science, circular economy, and smart technologies," *Food and Bioprocess Technology* 18(11), 9052-9108. https://doi.org/10.1007/s11947-025-04011-4

Marchese, A., Barbieri, R., Coppo, E., Orhan, I. E., Daglia, M., Nabavi, S. F., Izadi, M., Abdollahi, M., Nabavi, S. M., and Ajami, M. (2017). "Antimicrobial activity of eugenol and essential oils containing eugenol: A mechanistic viewpoint," *Critical Reviews in Microbiology* 43(6), 668-689. https://doi.org/10.1080/1040841X.2017.1295225

Martucci, J. F., Gende, L. B., Neira, L. M., and Ruseckaite, R. A. (2015). "Oregano and lavender essential oils as antioxidant and antimicrobial additives of biogenic gelatin films," *Industrial Crops and Products* 71, 205-213.

https://doi.org/10.1016/j.indcrop.2015.03.079
Mobilawon, F. E., Iroegbu, A. O. C., Zinyemba, O., and Meijboom, R. (2025). "Hydroxypropyl methylcellulose (HPMC) in sustainable pharmaceutical synthesis–Mechanistic insights, green metrics and outlook," *Sustainable Chemistry and Pharmacy* 48, article 102233. https://doi.org/10.1016/j.scp.2025.102233
Ncube, L. K., Ude, A. U., Ogunmuyiwa, E. N., Zulkifli, R., and Beas, I. N. (2020). "Environmental impact of food packaging materials: A review of contemporary development from conventional plastics to polylactic acid-based materials," *Materials* 13(21), article 4994. https://doi.org/10.3390/ma13214994
Ningtyas, R., Syahara, D. T., Nugraha, A. F., Saksono, N., and Chalid, M. (2025). "Lignin for food packaging: A review on its role as bio-based reinforcement and active functional material," *Bio-web EDP Sciences* 197(04004), 1-17. https://doi.org/10.1051/bioconf/202519704004
Nuñez, L., and D'Aquino, M. (2012). "Microbicide activity of clove essential oil (*Eugenia caryophyllata*)," *Brazilian Journal of Microbiology* 43, 1255-1260. https://doi.org/10.1590/S1517-83822012000400004
Oladzadabbasabadi, N., Manamperi, K., Dekiwadia, C., Murdoch, B. J., Hearn, K., Ghasemlou, M., Ivanova, E. P., and Adhikari, B. (2026). "Eco-friendly non-isocyanate polyurethane and carboxymethyl cellulose composite films reinforced with sodium lignosulfonate for sustainable packaging applications," *International Journal of Biological Macromolecules* (in press), 150548. https://doi.org/10.1016/j.ijbiomac.2026.150548
Otoni, C. G., Lorevice, M. V., de Moura, M. R., and Mattoso, L. H. C. (2018). "On the effects of hydroxyl substitution degree and molecular weight on mechanical and water barrier properties of hydroxypropyl methylcellulose films," *Carbohydrate Polymers* 185, 105-111. https://doi.org/10.1016/j.carbpol.2018.01.016
Öz, M., Fidan, M. S., Baltacı, C., Akmeşe, O., Sefalı, A., and Aygül, İ. (2026). "Chemical profiling of *Stachys cretica* subsp. *anatolica* Rech. f. (endemic) essential oils and their methanol extracts with evaluation as enzyme inhibitors, antioxidant, and antimicrobial agents," *BioResources* 21(1), 1274-1302. https://doi.org/10.15376/biores.21.1.1274-1302
Perone, N., Torrieri, E., Cavella, S., and Masi, P. (2014). "Effect of rosemary oil and HPMC concentrations on film structure and properties," *Food and Bioprocess Technology* 7(2), 605-609. https://doi.org/10.1007/s11947-012-1044-x
Reyes, D. C., Ma, Z., and Romero, J. J. (2024). "The antimicrobial properties of technical lignins and their derivatives—A review," *Polymers* 16(15), article 2181. https://doi.org/10.3390/polym16152181
Roy, S., Ramakrishnan, R., Goksen, G., Singh, S., and Łopusiewicz, Ł. (2024). "Recent progress on UV-light barrier food packaging films—A systematic review," *Innovative Food Science & Emerging Technologies* 91, article 103550. https://doi.org/10.1016/j.ifset.2023.103550
Rui, L., Li, Y., Wu, X., Wang, Y., and Xia, X. (2024). "Effect of clove essential oil nanoemulsion on physicochemical and antioxidant properties of chitosan film," *International Journal of Biological Macromolecules* 263, article 130286. https://doi.org/10.1016/j.ijbiomac.2024.130286
Ruwoldt, J., Blindheim, F. H., and Chinga-Carrasco, G. (2023). "Functional surfaces, films, and coatings with lignin—A critical review," *RSC Advances* 13(18), 12529-12553. https://doi.org/10.1039/d2ra08179b

Sayed, A., Safwat, G., Abdel-Raouf, M., and Mahmoud, G. A. (2023). "Alkali-cellulose/polyvinyl alcohol biofilms fabricated with essential clove oil as a novel scented antimicrobial packaging material," *Carbohydrate Polymer Technologies and Applications* 5, article 100273. https://doi.org/10.1016/j.carpta.2022.100273

Sharma, S., Barkauskaite, S., Jaiswal, A. K., and Jaiswal, S. (2021). "Essential oils as additives in active food packaging," *Food Chemistry* 343, article 128403. https://doi.org/10.1016/j.foodchem.2020.128403

Shi, R., and Li, B. (2016). "Preparation and characterization of corn starch and lignosulfonate blend film with a high content of lignosulfonate," *BioResources* 11(4), 8860-8874. https://doi.org/10.15376/biores.11.4.8860-8874

Silva, M. V., de Lima, A. D. C. A., Silva, M. G., Caetano, V. F., de Andrade, M. F., da Silva, R. G. C., de Moraes, L. E. P. T., de Lima Silva, I. D., and Vinhas, G. M. (2024). "Clove essential oil and eugenol: A review of their significance and uses," *Food Bioscience* 62, article 105112. https://doi.org/10.1016/j.fbio.2024.105112

Stoica, M., Bichescu, C. I., Crețu, C.-M., Dragomir, M., Ivan, A. S., Podaru, G. M., Stoica, D., and Stuparu-Crețu, M. (2024). "Review of bio-based biodegradable polymers: Smart solutions for sustainable food packaging," *Foods* 13(19), article e3027. https://doi.org/10.3390/foods13193027

Stoleru, E., and Brebu, M. (2021). "Stabilization techniques of essential oils by incorporation into biodegradable polymeric materials for food packaging," *Molecules* 26(20), article 6307. https://doi.org/10.3390/molecules26206307

Stramarkou, M., Oikonomopoulou, V., Missirli, T., Thanassoulia, I., and Krokida, M. (2020). "Encapsulation of rosemary essential oil into biodegradable polymers for application in crop management," *Journal of Polymers and the Environment* 28(8), 2161-2177. https://doi.org/10.1007/s10924-020-01760-5

Susilowati, M., Wahyuni, S., and Setiadi, A. (2025). "Morphological and yield traits of clove (*Syzygium aromaticum*) cultivated in South Sulawesi, Indonesia," *IOP Conference Series: Earth and Environmental Science* 012008. https://doi.org/10.1088/1755-1315/1469/1/012008

Tang, T., Fei, J., Zheng, Y., Xu, J., He, H., Ma, M., Shi, Y., Chen, S., and Wang, X. (2023). "Water-soluble lignosulfonates: Structure, preparation, and application," *ChemistrySelect* 8(13), article e202204941. https://doi.org/10.1002/slct.202204941

Tarhan, İ. (2021). "A robust method for simultaneous quantification of eugenol, eugenyl acetate, and β-caryophyllene in clove essential oil by vibrational spectroscopy," *Phytochemistry* 191, article 112928. https://doi.org/10.1016/j.phytochem.2021.112928

Tribot, A., Amer, G., Alio, M. A., de Baynast, H., Delattre, C., Pons, A., Mathias, J.-D., Callois, J.-M., Vial, C., and Michaud, P. (2019). "Wood-lignin: Supply, extraction processes and use as bio-based material," *European Polymer Journal* 112, 228-240. https://doi.org/10.1016/j.eurpolymj.2019.01.007

Tripathi, S., Kumar, L., Deshmukh, R. K., and Gaikwad, K. K. (2024). "Ultraviolet blocking films for food packaging applications," *Food and Bioprocess Technology* 17(6), 1563-1582. https://doi.org/10.1007/s11947-023-03221-y

Tundisi, L. L., Mostaço, G. B., Carricondo, P. C., and Petri, D. F. S. (2021). "Hydroxypropyl methylcellulose: Physicochemical properties and ocular drug delivery formulations," *European Journal of Pharmaceutical Sciences* 159, article 105736. https://doi.org/10.1016/j.ejps.2021.105736

Verma, C., Singh, V., and AlFantazi, A. (2024). "Cellulose, cellulose derivatives and cellulose composites in sustainable corrosion protection: Challenges and opportunities," *Physical Chemistry Chemical Physics* 26(15), 11217-11242. https://doi.org/10.1039/D3CP06057H

Vermeiren, L., Devlieghere, F., van Beest, M., de Kruijf, N., and Debevere, J. (1999). "Developments in the active packaging of foods," *Trends in Food Science & Technology* 10(3), 77-86. https://doi.org/10.1016/S0924-2244(99)00032-1

Xu, J. L., Lin, X., Wang, J. J., and Gowen, A. A. (2022). "A review of potential human health impacts of micro-and nanoplastics exposure," *Science of the Total Environment* 851(1), article 158111. https://doi.org/10.1016/j.scitotenv.2022.158111

Ye, D., Jiang, L., Hu, X., Zhang, M., and Zhang, X. (2016). "Lignosulfonate as reinforcement in polyvinyl alcohol film: Mechanical properties and interaction analysis," *International Journal of Biological Macromolecules* 83, 209-215. https://doi.org/10.1016/j.ijbiomac.2015.11.064

Zare, H. R., Jafari, S., Ghaffari, A., and Hassan, M. (2026). "Clove oil nanoemulsion: A proposed alternative to synthetic preservatives in pharmaceuticals, cosmetics and foods," *Journal of Food Measurement and Characterization* 20(2), 1880-1894. https://doi.org/10.1007/s11694-025-03679-8

Zhang, J., Wang, Q., Guo, W., Qin, Y., Hu, C., Zhang, K., Chang, J., Yu, X., Sun, L., and Fu, Q. (2025). "Transparent sodium lignosulfonate/phosphorylated sodium alginate/cellulose composite films with flame-retardant and UV-to-blue light-shielding performance," *ACS Applied Polymer Materials* 7(23), 16136-16151. https://doi.org/10.1021/acsapm.5c03406

Zor, M., Şen, F., Yazıcı, H., and Candan, Z. (2023). "Thermal, mechanical and morphological properties of cellulose/lignin nanocomposites," *Forests* 14(9), article 1715. https://doi.org/10.3390/f14091715

Zor, M., Yazici, H., Şen, F., Eroğlu, E., Candan, Z., and Rodrigue, D. (2024). "Preparation and characterization of hydroxyethyl cellulose/nanolignin composite films," *BioResources* 19(4), 7354-7365. https://doi.org/10.15376/biores.19.4.7354-7365

Article submitted: April 26, 2026; Peer review completed: June 8, 2026; Revised version received: July 20, 2026; Accepted: August 4, 2026; Published: August 19, 2026.
DOI: 10.15376/biores.21.4.9861-9879